CrossMark

On the Surface Helium Abundance of B-type Hot Subdwarf Stars from the WD+MS Channel of Type Ia Supernovae

Rui-Jie Ji[1,2,3,4], Xiang-Cun Meng[1,3,4], and Zheng-Wei Liu[1,3,4]

[1] Yunnan Observatories, Chinese Academy of Sciences, Kunming 650216, Kunming 650216, China; jiruijie@ynao.ac.cn, xiangcunmeng@ynao.ac.cn, zwliu@ynao.ac.cn
[2] University of Chinese Academy of Sciences, Beijing 100049, China
[3] Key Laboratory for the Structure and Evolution of Celestial Objects, Chinese Academy of Sciences, Kunming 650216, China
[4] International Centre of Supernovae (ICESUN), Yunnan Key Laboratory, Kunming 650216, China

Abstract

The origin of intermediate helium (He)-rich hot subdwarfs is still unclear. Previous studies have suggested that some surviving Type Ia supernovae (SNe Ia) companions from the white dwarf + main-sequence (WD+MS) channel may contribute to the intermediate He-rich hot subdwarfs. However, previous studies ignored the impact of atomic diffusion on the post-explosion evolution of surviving companion stars of SNe Ia, leading to the aspect that they could not explain the observed surface He abundance of intermediate He-rich hot subdwarfs. In this work, by taking the atomic diffusion and stellar wind into account, we trace the surviving companions of SNe Ia from the WD+MS channel using the one-dimensional stellar evolution code MESA until they evolve into hot subdwarfs. We find that the surface He-abundances of our surviving companion models during their core He-burning phases are in a range of $-1 \lesssim \log(N_{\mathrm{He}}/N_{\mathrm{H}}) \lesssim 0$, which are consistent with those observed in intermediate He-rich hot subdwarfs. This seems to further support the notion that it is possible for surviving companions of SNe Ia in the WD+MS channel to form some intermediate He-rich hot subdwarfs.

Key words: (stars:) subdwarfs – atomic processes – diffusion

1. Introduction

Because of their consistent peak luminosities, Type Ia supernovae (SNe Ia) are considered to be one of the most reliable distance indicators. As a result, SNe Ia are utilized to quantify cosmological parameters, which helped researchers reveal the Universe's rapid expansion. This suggests that dark energy is in charge of our Universe (Riess et al. 1998; Perlmutter et al. 1999). In order to evaluate the dark energy equation and its temporal evolution, SNe Ia are also employed as cosmic probes (Howell 2011; Sullivan et al. 2011).

Even though SNe Ia are crucial to contemporary astrophysics, there is ongoing discussion over a few fundamental issues, including their progenitor systems and explosion mechanism (Hillebrandt & Niemeyer 2000; Leibundgut 2000; Wang & Han 2012; Maoz et al. 2014; Liu et al. 2023). The majority of researchers agree that a close binary which includes one carbon–oxygen white dwarf (CO WD) is where supernovae (SNe) Ia start (Hillebrandt & Niemeyer 2000; Branch 2004; Nugent et al. 2011; Hillebrandt et al. 2013). Thus, the progenitor models of SNe Ia are primarily separated into the single-degenerate (SD) model and the double-degenerate (DD) model based on the different sorts of companions (Whelan & Iben 1973; Nomoto 1982; Iben & Tutukov 1984; Webbink 1984). The non-degenerate

companion star in the SD model could be a main-sequence star (i.e., the WD+MS channel), a sub-giant, a red giant star (i.e., the WD+RG channel), an asymptotic giant branch star (i.e., the WD+AGB channel), or a helium star (i.e., the WD+He star channel) (Whelan & Iben 1973; Nomoto et al. 1984; Wang et al. 2009; Wang & Han 2012; Li et al. 2023). The binary system in the DD model is made up of two CO WDs (Han 1998; Liu et al. 2018). While no surviving companion is left in the standard DD model, the SD model predicts that the companion stars will survive after the SN Ia explosion. Finding the surviving companions in nearby SN remnants is therefore a promising way to differentiate between the SD and DD models. As a consequence, a detailed analysis of the characteristics of the potential surviving companions is believed to be useful in understanding the origins of SNe Ia (Li et al. 2017; Meng & Li 2019; Ruiz-Lapuente 2023).

Hot subdwarfs have been proposed to be possible candidates of surviving companions of SNe Ia (e.g., Meng & Li 2019). They are core helium-burning stars with a very thin hydrogen envelope, and they are generally divided into B-type hot subdwarf stars (sdBs) and O-type hot subdwarf stars (sdOs) according to their spectral features (Green et al. 1986). In the Hertzsprung–Russell (HR) diagram, hot subdwarfs are either located at the blue end of the horizontal branch (HB) or have evolved past that stage (Heber 2009). SdBs typically have

effective temperatures between 20,000 and 40,000 K, while sdOs have effective temperatures between 40,000 and 80,000 K, and are generally more luminous than sdBs. Some mysteries regarding the genesis of hot subdwarfs remain. Given that a significant portion of sdB stars are found in close binaries, processes involving binary interaction should be responsible for their formation (Heber 2009, 2016). A detailed description of how hot subdwarfs originate via binary evolution, specifically through the channels of Roche Lobe overflow (RLOF), common envelope (CE) ejection and double He WDs merger, can be found in Han et al. (2002, 2003).

Most hot subdwarfs are observed to present some peculiar chemical abundance signatures. The majority of sdBs have a He deficient atmosphere, and their surface He abundance may be as little as a thousandth of the solar value. From one percent of the solar value to nearly pure He atmosphere, the sdOs display a range of surface He abundances (Heber 2009, 2016). Previous researchers have categorized hot subdwarfs into He-deficient and He-rich hot subdwarfs based on the solar helium abundance $\log(N_{He}/N_H) = -1$, where N_H and N_{He} represent the surface number densities of hydrogen and helium, respectively (Németh et al. 2012; Luo et al. 2016, 2019). He-rich hot subdwarfs are further divided into extreme He-rich (eHe-rich) stars $(\log(N_{He}/N_H) > 0)$ and intermediate He-rich (iHe-rich) stars $(-1 < \log(N_{He}/N_H) < 0)$. Generally, it is believed that the He-rich group results from the merger of two He WDs, whereas the He-deficient group most likely originates from the RLOF and CE ejection channels (Han et al. 2002, 2003; Heber 2009, 2016). However, it is still unclear where the iHe-rich group originated (Martin et al. 2017; Luo et al. 2019).

Meng & Podsiadlowski (2017) proposed a new version of SD model for SN Ia, i.e., the common-envelope wind (CEW) model. In the model, if the mass transfer rate between a CO WD and its companion exceeds a critical accretion rate, a CE forms around the binary system. The WD may gradually increase its mass at the base of the CE. Based on the CEW model, Meng & Luo (2021) studied the formation of hot subdwarfs from the surviving companions of SNe Ia in the WD+MS channel (Meng & Li 2019; Meng et al. 2020), and then compared their results with some observational properties of iHe-rich hot subdwarfs. They discovered that several observational features, such as their effective temperatures and surface gravities, may be explained by the hot subdwarfs from this channel. However, it is still difficult for their models to explain the observed surface He-abundances of iHe-rich subdwarfs. This may be because the effect of the atomic diffusion and wind mass loss from the surface of the sdB star was ignored in their calculations.

Previous studies have shown that the the atomic diffusion and wind mass loss from the surface of an sdB star could considerably affect its surface He abundances (Unglaub & Bues 2001; Hu et al. 2011). Therefore, it will be still important

to investigate whether or not the inclusion of the atomic diffusion and wind mass loss during the evolution of surviving companion stars of SNe Ia in the WD+MS channel could explain the observed surface He-abundance of iHe-rich subdwarfs. Therefore, by taking the atomic diffusion and stellar wind into account, we follow the evolution of SNe Ias' surviving companions from the WD+MS channel until they evolve hot subdwarfs using the one-dimensional stellar evolution code Modules for Experiments in Stellar Astrophysics (MESA) in this work. We describe our methods in Section 2. Section 3 displays the results, while Section 4 provides the discussions and summaries.

2. Methods

2.1. Atomic Diffusion

The phrase "atomic diffusion" refers to a group of particle transport mechanisms that alter a star's chemical composition. Radiative levitation, thermal diffusion, concentration diffusion and gravitational settling are some of these mechanisms (Hu et al. 2010). The rivalry between outward radiant forces and inward gravity determines an element's actual diffusion velocity, which varies depending on the element (Hu et al. 2010, 2011). As such, the abundance profile of a star is directly impacted by atomic diffusion (Byrne et al. 2018). Because the diffusion timescale is roughly proportional to the density of protons, atomic diffusion is more efficient in a star's outer layers (Deal et al. 2018). Consequently, atomic diffusion must be included in order to accurately forecast surface abundance, particularly for stars with high surface gravity like hot subdwarfs (Campilho et al. 2022).

The atomic diffusion in a hot subdwarf from the WD+MS SN Ia channel is studied using the stellar evolution code MESA. MESA includes concentration diffusion, thermal diffusion and gravitational settling as the standard processes with the *do_element_diffusion* flag. In MESA, the atomic diffusion is computed by the use of the Thoul et al. (1994) and Hu et al. (2011) formalism to solve the Burgers equations (Burgers 1969). The radiative levitation is included as an optional method (Paxton et al. 2011, 2013, 2015, 2018, 2019). In this paper, we just focus on the surface helium abundance. Generally, the effect of radiative levitation on the helium is not significant, but is remarkable to heavy elements (Hu et al. 2010, 2011). Thus, we do not take into account the effect of radiation levitation in this study since calculating radiative levitation in MESA takes a lot of time.

2.2. Subdwarf Models

In the WD+MS channel, a WD accretes hydrogen-rich materials from the companion star when the companion fills its Roche lobe on the MS or in the Hertzsprung gap (HG) (Meng & Podsiadlowski 2017). The WD explodes as an SN Ia when
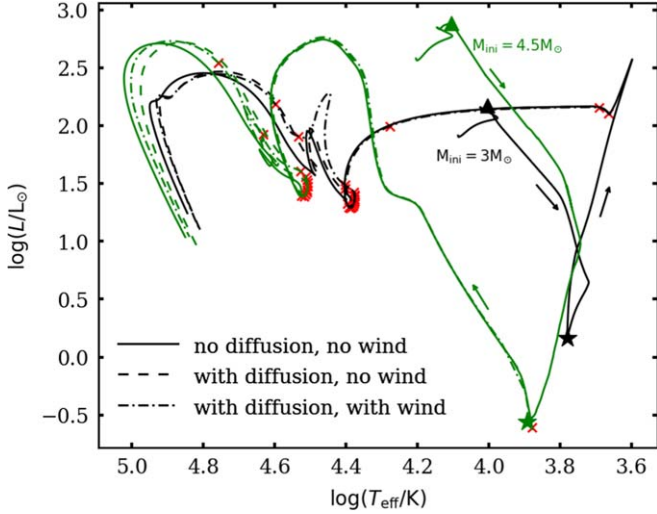
Figure 1. The evolutionary tracks of two companion stars with initial mass of $3\,M_\odot$ (black lines, model A) and $4.5\,M_\odot$ (green lines, model B) in the HR diagram. The triangles represent the position where the companions start to lose mass. The asterisks represent the position where an SN Ia explosion is assumed. The arrows indicate the evolutionary direction. The age gap in each line between two consecutive red crosses is 10^7 yr.

its mass exceeds the Chandrasekhar mass limit. The companion may continue to evolve into an sdB star. Since we are only concerned with the surface helium abundance of the companion star during the sdB phase, we use single-star evolution instead of binary evolution calculation to construct sdB models. The mass transfer of the companion is then modeled with a constant mass-loss rate.

For systems with different initial masses, we display the evolution of the models in the HR diagram in Figure 1. First, we choose two MS stars of $3\,M_\odot$ (model A) and $4.5\,M_\odot$ (model B) with solar abundances ($X = 0.70$, $Y = 0.28$, $Z = 0.02$), and evolve them to the stage of the HG phase. Then, we activate the high mass-loss rate option (the *mass_change* option in MESA) to simulate the mass loss of the star. For model A, the mass loss timescale is 2.5×10^6 yr, and the mass loss rate is $10^{-6}\,M_\odot$ yr^{-1}. For model B, the mass loss timescale is 3.98×10^5 yr, and the mass loss rate is $10^{-5}\,M_\odot$ yr^{-1}. Then, we assume an SN Ia occurs and the mass loss stops. The systems with a more massive WD, and more massive companion, are more likely to form hot subdwarfs, which mean a higher mass loss rate and then a shorter mass loss rate. The employed mass loss timescale and mass loss rate used here are comparable to those of typical binary evolutions for SNe Ia (Meng & Podsiadlowski 2017), and the hot subdwarf stars from such a treatment are similar to those from a system with ($\log P^{\mathrm{i}}/\mathrm{days}$, $M_{\mathrm{WD}}^{\mathrm{i}}/M_\odot$) = (0.5, 1.1) (Meng & Luo 2021). During the mass loss phase, the companion stars lose almost all of their hydrogen envelope, which makes the diffusion effect insignificant. Then, before the SN explosion, we do not consider the atomic diffusion process in our models.

During the following evolution, we carry out three cases with different physical inputs. Models A0/B0 do not include the atomic diffusion and the stellar wind, i.e., similar to that in Meng & Luo (2021). Models A1/B1 only include the atomic diffusion, and models A2/B2 include both the atomic diffusion and the stellar wind. We use the Reimers' wind to simulate the wind mass loss from the surface of the surviving companion, where η_{Reimers} is set to 0.1 (Reimers 1975).

3. Results

3.1. Evolution to the sdB

After the rapid mass loss phase, the masses of models A and B are $0.5\,M_\odot$ and $0.52\,M_\odot$, respectively, and the hydrogen envelope masses are $0.2\,M_\odot$ and $0.02\,M_\odot$, respectively. The following evolutions of the stars are also shown in Figure 1. For model A, the star consecutively experiences the red giant branch and the HB phases. Its hydrogen envelope is consumed by shell hydrogen burning during the HB phase, causing the envelope to grow gradually thinner. For the consumption of the envelope, its surface temperature becomes higher and higher, and then, the star evolves to the hot subdwarf stage in the HR diagram. After the exhaustion of the helium in the core, the subdwarf directly evolves to the WD branch, rather than to the AGB. For model B, the star will expand rapidly, and then enter the sdB stage about two million years after mass loss is stopped (see also in Meng et al. 2020). Due to its larger mass, model B has a higher surface effective temperature compared to model A during the sdB phase. Its subsequent evolution track is similar to model A. The differing post-SN Ia evolutions of models A and B may be traced back to the varying masses of the hydrogen-rich envelope when the supernova explosion occurs; in other words, the evolution track of a star with a thicker hydrogen envelope is more similar to that of an isolated star.

We present the evolution of the companions in the $\log g - \log T_{\mathrm{eff}}$ diagram in Figure 2 in order to compare with observations, where some iHe-rich subdwarfs are also shown and the observational data are from Lei et al. (2018, 2019, 2020) and Luo et al. (2019, 2021). The iHe-rich hot subdwarf samples shown here are isolated stars. As demonstrated in Figure 1, different physical inputs cannot affect the evolutions of the surviving companions in the $\log g - \log T_{\mathrm{eff}}$ diagram. Figure 2 shows that the evolutionary tracks span several regions of iHe-rich hot subdwarfs, i.e., the surviving companion model may explain several observational properties of the iHe-rich subdwarfs as suggested by Meng & Luo (2021). In fact, the initial binary parameters of the systems generating SNe Ia largely determine the features of hot subdwarfs from the WD+MS channel. Meng & Luo (2021) studied many hot subdwarf models from the WD+MS channel with different initial masses and orbital periods. If the initial orbital period is longer (mass transfer occurs relatively later) and the initial
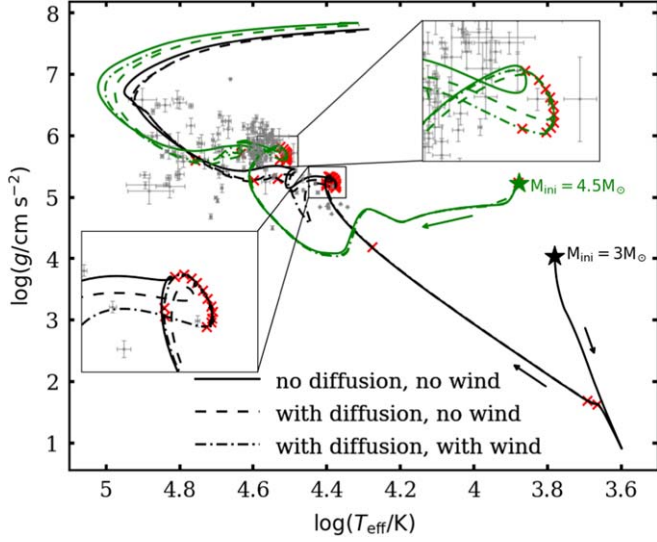
Figure 2. The evolutionary tracks of two companion stars with initial mass of $3\,M_\odot$ (black lines, model A) and $4.5\,M_\odot$ (green lines, model B) in a $\log g - \log T_{\rm eff}$ diagram. The asterisks represent the position where an SN Ia explosion is assumed. The arrows represent the evolutionary direction. The age gap in each line between two consecutive red crosses is 10^7 yr. The gray dots belong to the iHe-rich group, and the data are from Lei et al. (2018, 2019, 2020) and Luo et al. (2019, 2021).

mass of the companion star is larger (the surviving companion may be relatively more massive), the companion may have a higher effective temperature and a higher surface gravity in the hot subdwarf phase. Additionally, we notice that the evolution track of models A1/B1 (dashed line) is somewhat pushed to lower surface gravities and effective temperatures when compared to models A0/B0 (solid line). This is because of the outward diffusion of H, which is followed by a drop in envelope density. As a result, the sdB star becomes somewhat bigger and colder, and the envelope becomes less gravitationally bound. However, the difference is so insignificant that it cannot be discriminated by observations. Therefore, the location of the hot subdwarf stars in the HR or $\log g - \log T_{\rm eff}$ diagrams is not much affected by atomic diffusion, at least for those from the SN Ia channel.
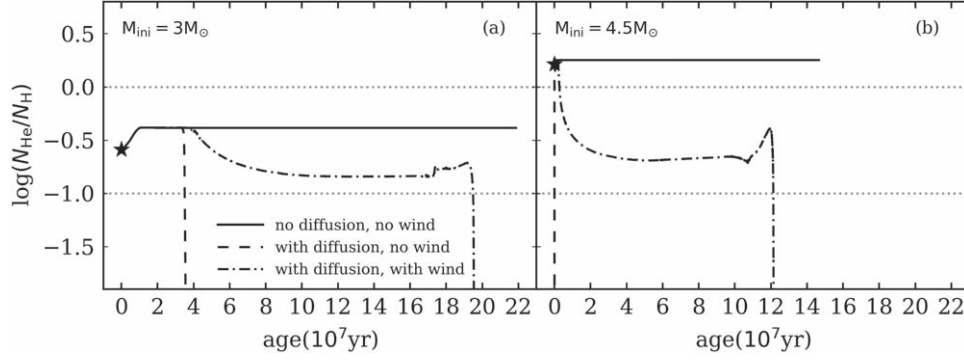
3.2. Surface Helium Abundance

After the supernova explosions, the surface helium abundances for the models A and B are about $\log(N_{\rm He}/N_{\rm H}) = -0.59$ and $\log(N_{\rm He}/N_{\rm H}) = 0.24$, respectively. The following evolution of $\log(N_{\rm He}/N_{\rm H})$ depends on the physical inputs and the evolutionary stage the stars are experiencing. In Figure 3, we show the evolutions of $\log(N_{\rm He}/N_{\rm H})$ for model A (panel (a)) and model B (panel (b)), where the surface number densities of hydrogen and helium are denoted by $N_{\rm H}$ and $N_{\rm He}$, respectively. In panel (a), there is an increase in surface helium abundance for model A due to the first dredge up in the RG phase, where the atomic

diffusion does not take effect until the surface convection ceases. Model B does not experience the RG stage, and then, the atomic diffusion takes effect immediately, as shown in panel (b) of Figure 3. For models A0/B0 (solid line), the surface helium and hydrogen abundances are not changed during the whole subdwarf stage and the surface helium abundance of model A0 is consistent with the iHe-rich hot subdwarfs from observation. For models A1/B1 (dashed line), as shown in previous studies (Wesemael et al. 1982; Fontaine & Chayer 1997), the helium on the surface quickly settles down below the photosphere within about 10^4 yr for the effect of gravitational settling, and the surface almost becomes a pure hydrogen atmosphere, i.e., $\log(N_{\rm He}/N_{\rm H})$ becomes lower than 10^{-15}. Then in Figure 3, we do not show the whole range of $\log(N_{\rm He}/N_{\rm H})$ for models A1/B1. For models A2/B2 (dot–dashed line), the helium will also settle down as in models A1/B1. However, $\log(N_{\rm He}/N_{\rm H})$ will stay at a level between 0 and -1 for about 1.8×10^8 yr for model A2 and 1×10^8 yr for model B2 due to the presence of stellar wind, until the stars evolve to the WD branch. In other words, the stars behave as iHe-rich subdwarfs.

Actually, the surface helium abundance during the hot subdwarfs heavily depends on the mass of the remaining hydrogen-rich envelope after the SN explosion; usually, the less massive the envelope, the higher the surface helium abundance in the sdB phase. To compare with the observations of iHe-rich hot subdwarfs, we demonstrate the evolution of models A2/B2 in the $\log(T_{\rm eff}) - \log(N_{\rm He}/N_{\rm H})$ diagram in Figure 4. This figure represents the companions following the supernova explosion spend most of their time in the area of iHe-rich hot subdwarfs, if the effect of atomic diffusion and stellar wind are considered. Again, the parameter of the initial model has a great influence on the position in $\log(T_{\rm eff}) - \log(N_{\rm He}/N_{\rm H})$ plane for our models.

3.3. Helium Abundance Profile

The He-profile versus the fractional mass $\log(1 - m/M)$ at three different ages of the companion stars—1×10^7, 3×10^7 and 5×10^7 yr after the supernova explosion—is shown in Figure 5 to demonstrate the influence of a time-dependent diffusion. Without the atomic diffusion, the helium abundance does not change in the envelope, as shown in panels (A0)/(B0) of Figure 5. The outward movement of the helium core is due to the burning of the hydrogen shell. If we consider the diffusion only, the surface helium settles down quickly and the outer layer consists of pure hydrogen. In particular, the outer hydrogen envelope becomes thicker and thicker as shown in panels (A1)/(B1). If both atomic diffusion and stellar wind are considered, although the surface helium will settle down, the stellar wind will simultaneously peel off the outer layer, and then the surface helium abundance can remain at relatively high level, as demonstrated in panels (A2)/(B2). The figure also

Figure 3. The evolution of $\log(N_{He}/N_H)$ with time, where the surface number densities of hydrogen and helium are denoted by N_H and N_{He}, respectively. The range of He abundance for iHe-rich hot subdwarfs is shown by the two dotted lines. The asterisks represent the position where an SN Ia explosion is assumed.
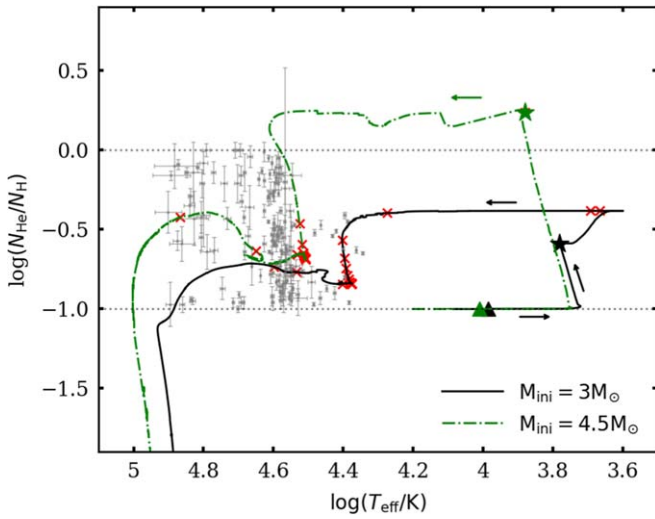
Figure 4. The evolution of $\log(T_{eff})$ and $\log(N_{He}/N_H)$ in models with diffusion and wind. The arrows represent the evolutionary direction, and the asterisks represent the position where an SN Ia explosion is assumed. The age gap in each line between two consecutive red crosses is 10^7 yr. The range of He abundance for iHe-rich hot subdwarfs is shown by the two dotted lines. The gray dots belong to the iHe-rich group, and the data are from Lei et al. (2018, 2019, 2020) and Luo et al. (2019, 2021).

makes it very clear that the interior profile is seldom impacted by atomic diffusion, and that atomic diffusion works well only in the outer layer, which makes up around 1% mass of the star.

4. Discussion and Summary

Following Meng & Luo (2021), we used MESA to compute different hot subdwarf models with or without the effects of the atomic diffusion and the stellar wind. For the basic models with no diffusion, if the surface convention ceases, surface helium abundance remains constant after supernova explosion. With the atomic diffusion included, surface helium is depleted quickly when the surface convection ceases. However, if a stellar wind is also included, the surface helium abundance can stay at the iHe-rich level during the whole sdB phase.

To simplify the calculation, we used single star evolution to replace binary evolution in this paper. Therefore, we have ignored some interactions in binary evolution, which may have some impact on our results. For example, in binary evolution, the ejecta from a supernova explosion can strip away portions of the envelope of the companion star (Marietta et al. 2000; Meng et al. 2007; Pan et al. 2010; Liu et al. 2012; Bauer et al. 2019; McCutcheon et al. 2022), which might lead to a slight increase in the surface helium abundance of the companion (see also the discussion in Meng et al. 2020). In this paper, we just evolve two models, because the calculation of the atomic diffusion is a very time-consuming task in MESA. However, Meng & Luo (2021) studied many star models from the WD +MS channel, and different initial masses and orbital periods are taken into account in detail. In the $\log g - \log T_{eff}$ diagram, their models could cover most samples of the iHe-rich hot subdwarfs. The basic conclusions based on the two models may not be changed by different initial models. In addition, we used the Remiers' wind as the mass-loss rate in our model. The physics of the wind of hot subdwarfs may be complex (Krtička et al. 2016). We did some tests with stellar wind of different constant mass loss rates, an approach which is similar to testing different stellar wind coefficients, and found that the weaker the stellar wind, the lower the surface helium abundance of our model in the hot subdwarf phase. Thus, different stellar wind models and wind coefficients could produce hot subdwarfs with different surface abundances, which need to be studied in more detail in the future. Moreover, the abundance of surface elements is not only affected by the stellar wind and the atomic diffusion, but also affected by other physical mechanisms, such as surface rotation, magnetic field, turbulent mixing, etc. For example, in the work of Hu et al. (2011), they studied a typical hot subdwarf of $0.46\,M_\odot$, with mixing of the outer $\Delta M \approx 10^{-8}$, 10^{-7} and $10^{-6}\,M_\odot$, respectively. Their models reproduced the observed He abundances of He-deficient ones.
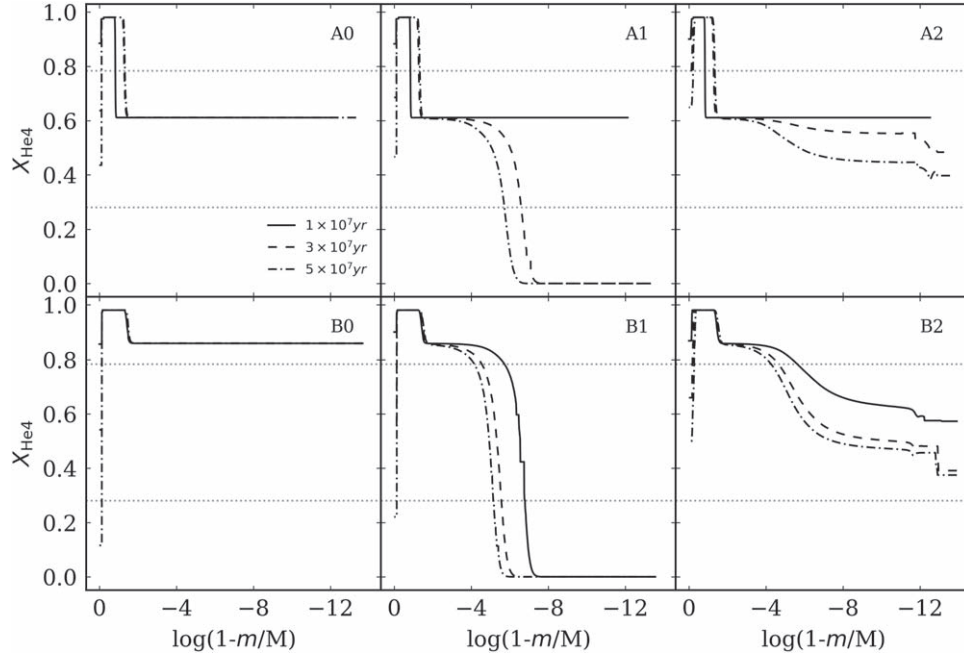
Figure 5. Snapshots of the helium abundance profile for different models. Different lines represent different time points after the SN Ia explosion. The range of He abundance for iHe-rich hot subdwarfs is shown by the two dotted lines.

Though a few evolutionary situations about iHe-rich hot subdwarfs have been proposed, including the merging of a low-mass MS star with a He WD (Zhang et al. 2017), a post-CE system with incomplete atmosphere stratification (Naslim et al. 2012), the late hot-flasher scenario (Miller Bertolami et al. 2008), the formation of iHe-rich cases remains unclear. As described in Meng & Luo (2021), the atmosphere of the companion may be polluted by supernova ejecta. As a result, the iron-peak elements could be enhanced on the surface of the hot subdwarfs from the supernova channel. It must be noted that the SN Ia channel provides just part of the iHe-rich hot subdwarfs with specific Galactic kinematic features, so it is not possible to be the main contributor. Thus, the origin of iHe-rich hot subdwarfs and the physical mechanisms affecting the helium abundance on the surface of hot subdwarfs remain to be investigated in detail.

Acknowledgments

References

Bauer, E. B., White, C. J., & Bildsten, L. 2019, ApJ, 887, 68
Branch, D. 2004, Natur, 431, 1044
Burgers, J. M. 1969, Flow Equations for Composite Gases (New York: Academic)
Byrne, C. M., Jeffery, C. S., Tout, C. A., & Hu, H. 2018, MNRAS, 475, 4728
Campilho, B., Deal, M., & Bossini, D. 2022, A&A, 659, A162
Deal, M., Alecian, G., Lebreton, Y., et al. 2018, A&A, 618, A10
Fontaine, G., & Chayer, P. 1997, in The Third Conf. on Faint Blue Stars, ed. A. G. D. Philip et al., 169
Green, R. F., Schmidt, M., & Liebert, J. 1986, ApJS, 61, 305
Han, Z. 1998, MNRAS, 296, 1019
Han, Z., Podsiadlowski, P., Maxted, P. F. L., & Marsh, T. R. 2003, MNRAS, 341, 669
Han, Z., Podsiadlowski, P., Maxted, P. F. L., Marsh, T. R., & Ivanova, N. 2002, MNRAS, 336, 449
Heber, U. 2009, ARA&A, 47, 211
Heber, U. 2016, PASP, 128, 082001
Hillebrandt, W., Kromer, M., Röpke, F. K., & Ruiter, A. J. 2013, FrPhy, 8, 116
Hillebrandt, W., & Niemeyer, J. C. 2000, ARA&A, 38, 191
Howell, D. A. 2011, NatCo, 2, 350
Hu, H., Glebbeek, E., Thoul, A. A., et al. 2010, A&A, 511, A87
Hu, H., Tout, C. A., Glebbeek, E., & Dupret, M. A. 2011, MNRAS, 418, 195
Iben, I. J., & Tutukov, A. V. 1984, ApJS, 54, 335
Krtička, J., Kubát, J., & Krtičková, I. 2016, A&A, 593, A101
Lei, Z., Zhao, J., Németh, P., & Zhao, G. 2018, ApJ, 868, 70
Lei, Z., Zhao, J., Németh, P., & Zhao, G. 2019, ApJ, 881, 135
Lei, Z., Zhao, J., Németh, P., & Zhao, G. 2020, ApJ, 889, 117
Leibundgut, B. 2000, A&ARv, 10, 179

Li, C.-J., Chu, Y.-H., Gruendl, R. A., et al. 2017, ApJ, 836, 85
Li, L.-H., Liu, D.-D., & Wang, B. 2023, RAA, 23, 075010
Liu, D., Wang, B., & Han, Z. 2018, MNRAS, 473, 5352
Liu, Z. W., Pakmor, R., Röpke, F. K., et al. 2012, A&A, 548, A2
Liu, Z.-W., Röpke, F. K., & Han, Z. 2023, RAA, 23, 082001
Luo, Y., Németh, P., Deng, L., & Han, Z. 2019, ApJ, 881, 7
Luo, Y., Németh, P., Wang, K., Wang, X., & Han, Z. 2021, ApJS, 256, 28
Luo, Y.-P., Németh, P., Liu, C., Deng, L.-C., & Han, Z.-W. 2016, ApJ, 818, 202
Maoz, D., Mannucci, F., & Nelemans, G. 2014, ARA&A, 52, 107
Marietta, E., Burrows, A., & Fryxell, B. 2000, ApJS, 128, 615
Martin, P., Jeffery, C. S., Naslim, N., & Woolf, V. M. 2017, MNRAS, 467, 68
McCutcheon, C., Zeng, Y., Liu, Z. W., et al. 2022, MNRAS, 514, 4078
Meng, X., Chen, X., & Han, Z. 2007, PASJ, 59, 835
Meng, X., & Li, J. 2019, MNRAS, 482, 5651
Meng, X., & Podsiadlowski, P. 2017, MNRAS, 469, 4763
Meng, X.-C., Han, Z.-W., Podsiadlowski, P., & Li, J. 2020, ApJ, 903, 100
Meng, X.-C., & Luo, Y.-P. 2021, MNRAS, 507, 4603
Miller Bertolami, M. M., Althaus, L. G., Unglaub, K., & Weiss, A. 2008, A&A, 491, 253
Naslim, N., Geier, S., Jeffery, C. S., et al. 2012, MNRAS, 423, 3031
Németh, P., Kawka, A., & Vennes, S. 2012, MNRAS, 427, 2180
Nomoto, K. 1982, ApJ, 253, 798

Nomoto, K., Thielemann, F. K., & Yokoi, K. 1984, ApJ, 286, 644
Nugent, P. E., Sullivan, M., Cenko, S. B., et al. 2011, Natur, 480, 344
Pan, K.-C., Ricker, P. M., & Taam, R. E. 2010, ApJ, 715, 78
Paxton, B., Bildsten, L., Dotter, A., et al. 2011, ApJS, 192, 3
Paxton, B., Cantiello, M., Arras, P., et al. 2013, ApJS, 208, 4
Paxton, B., Marchant, P., Schwab, J., et al. 2015, ApJS, 220, 15
Paxton, B., Schwab, J., Bauer, E. B., et al. 2018, ApJS, 234, 34
Paxton, B., Smolec, R., Schwab, J., et al. 2019, ApJS, 243, 10
Perlmutter, S., Aldering, G., Goldhaber, G., et al. 1999, ApJ, 517, 565
Reimers, D. 1975, MSRSL, 8, 369
Riess, A. G., Filippenko, A. V., Challis, P., et al. 1998, AJ, 116, 1009
Ruiz-Lapuente, P. 2023, FrASS, 10, 1112880
Sullivan, M., Guy, J., Conley, A., et al. 2011, ApJ, 737, 102
Thoul, A. A., Bahcall, J. N., & Loeb, A. 1994, ApJ, 421, 828
Unglaub, K., & Bues, I. 2001, A&A, 374, 570
Wang, B., & Han, Z. 2012, NewAR, 56, 122
Wang, B., Meng, X., Chen, X., & Han, Z. 2009, MNRAS, 395, 847
Webbink, R. F. 1984, ApJ, 277, 355
Wesemael, F., Winget, D. E., Cabot, W., van Horn, H. M., & Fontaine, G. 1982, ApJ, 254, 221
Whelan, J., & Iben, I. J. 1973, ApJ, 186, 1007
Zhang, X., Hall, P. D., Jeffery, C. S., & Bi, S. 2017, ApJ, 835, 242